2024-26-0060 Published 16 Jan 2024

Exploring Capabilities of Hydraulic Actuators to Achieve Vehicle Ride Targets in Frequency Range beyond Their Operational Bandwidth

Ayush Agrawal, Ayush Negi, and Divyanshu Joshi Jaguar Land Rover TBSI Pvt. Ltd.

Citation: Agrawal, A., Negi, A., and Joshi, D., "Exploring Capabilities of Hydraulic Actuators to Achieve Vehicle Ride Targets in Frequency Range beyond Their Operational Bandwidth," SAE Technical Paper 2024-26-0060, 2024, doi:10.4271/2024-26-0060.

Received: 04 Sep 2023 Revised: 15 Sep 2023 Accepted: 25 Oct 2023

Abstract

Active suspension systems employ sophisticated control algorithms to deliver superior comfort in vehicles. However, the capabilities of these algorithms are limited by the physical constraints of actuators. Many vehicles use hydraulic actuators in their active suspension system, which use fluid movement to control suspension motion. These systems inherently have slower response times due to the nature of fluid flow and the time required to build up or release pressure within the hydraulic system. Typically, hydraulic systems operate in a low bandwidth of 0-5 Hz. This limits their capability to only meeting vehicle's primary ride targets which typically lie below 5 Hz. Although they can be tuned to operate at a slightly higher frequency range (up to 10 Hz), they perform poorly in attenuating the secondary ride vibration, i.e., 5 – 25 Hz. This paper focuses on investigating the possible hardware and subsequently control capabilities that can allow us to affect the vehicle ride well beyond the actuator bandwidth. The aim is to conduct a detailed simulation-based analysis to investigate the possibility of expanding the effective operational frequency range of hydraulic actuators. In this work, we studied force applications in the frequency range of 0 - 5 Hz with different amplitudes at four corner modules and evaluated the ride performance using Fast Fourier Transformation (FFT). This paper concludes with a discussion about the extent of Hydraulic Actuator limitations and the required technological advancements for improving the secondary ride response.

Introduction

Enhancement in ride and handling constantly demands evolution in suspension technology. Active suspension system is one such technology that has attracted every OEM's attention since its introduction on an F1 car named "Lotus type 92" in 1983. The technology promises superior ride and handling if sophisticated actuators (hardware) and advanced control logic (software) are engineered to meet the ride and handling targets.

There are three categories of active actuators: Electromagnetic Actuators, Hydraulic Actuators, and Pneumatic Actuators. After the debut of *MultiMatic's TrueActive*™ *Spool Valve* (TASV) Damper on the Ferrari Purosangue in 2022 [1], electric actuators have gained substantial attention in the automotive industry. However, OEMs outside ultra-luxury segment refrain from installing this extremely costly hardware on their vehicles. Auto manufacturers such as Audi, BMW, and Mercedes-Benz use air springs (pneumatic actuators) in their adaptive or active suspension system [2]. These premium vehicles are laden with numerous features resulting in a heavy mass vehicle unlikely to be controlled using limited force capability and short life cycle of pneumatic suspension. For these reasons, hydraulic suspensions with their high power-to-weight ratio make them apt for active suspension system [3].

Researchers have developed and implemented several control schemes for the control of hydraulic actuators in active suspension. Some control schemes that have been explored comprehensively in literature are linear-quadratic regulator (LQR) [4], H_∞ control [5] [6], and preview control using Model Predictive Control (MPC) [7]. Authors in [5] have developed a finite-frequency H_∞ controller to suppress the sprung vibration in the frequency range 4 – 8 *Hz*. The research [5] adopts a full-car model while considering parametric uncertainties, suspension deflection constraints, and actuation constraints. The algorithm apparently improves the vehicle ride in the frequency range 4 – 8 *Hz*, however fails to ameliorate the primary ride (0 – 4*Hz*). The finite operational bandwidth characteristics of actuators in their model are not included and hence present no evidence of ride improvement in such pragmatic scenarios. Similar research has been conducted in [6], where a constrained H_∞ controller has been developed for a to solve the same constrained problem, but with a focus of striking a perfect

balance between passenger comfort and handling. We believe if hydraulic actuators were considered in the system modelling, the proposed algorithms might have failed due to nonlinear characteristics of the hydraulic circuit. Online optimization techniques like Model Predictive Control (MPC) have been utilized in [7] with a focus to improve only vehicle ride. Authors in [7] use a reduced full car model excluding wheel dynamics because low operational bandwidth of actuators cannot influence wheel motion. They do consider nonlinearity of the vehicle model along with all constraints as presented in [5] [6], but do not include actuator dynamics in their design problem.

Similar to new reforms in control logics (software), researchers do emphasize on designing more capable actuators (hardware) for active suspension technology. Two such developments are (a) electromagnetic-pneumatic actuator for high bandwidth applications [8], (b) low bandwidth actuator with continuously variable damper [4]. The proposed electromagnetic-pneumatic actuator in [8] are heavy and have large volume, much the same as hydraulic/pneumatic actuators. In addition to this, these actuators have smaller force densities compared to hydraulic, pneumatic and piezoelectric actuators. In [4], the researchers have proposed an energy efficient and cost-effective low bandwidth actuator with continuous variable damper. A schematic of the same is presented in Fig. 1(b). They reported a 43% increase in ride response by combining the continuous variable damper and LBAS system with a 3*Hz* cut-off frequency. These conclusions were made by simulating the proposed actuator with a quarter car model.

Human beings are most sensitive in the range $4-8$ *Hz* for vertical motion, and $1-2$ *Hz* for the horizontal motion [9]. Therefore, it is crucial to consider pitch and roll dynamics to comprehensively analyze the ride performance of any newly proposed suspension technology. Hence, we use full-car model in our study. If a 43% increase in ride response is achievable using LBAS system with 3*Hz* cutoff frequency, as reported in [4], then there exists a possibility to achieve a similar or even better ride performance with a hydraulic actuator installed in a HBAS system, see Fig. 1(c). Moreover, [10] reports that vertical vibrations in the chassis, up to 5 Hz, can be actively damped by low bandwidth hydraulic systems. These findings motivate us to further explore the potential of hydraulic actuators in HBAS system by reinvestigating the vehicle ride characteristics under its action. Improvements in ride response beyond 5 *Hz* will fuel our motivations further to develop novel control strategies for hydraulic active suspension systems.

We organize the rest of our work in the following sections to answer this question. In Section II, we outline the specifics of the vehicle model utilized in conducting simulations in our study, and formally define the problem statement. In Sec.III, we conduct the simulations and present main results addressing the problem statement. In Sec.IV, we draw some conclusions & discuss future aspects of the work.

FIGURE 1 (a) Passive (b) Low Bandwidth Suspension System (LBAS) (c) High Bandwidth Suspension System (HBAS) [6]

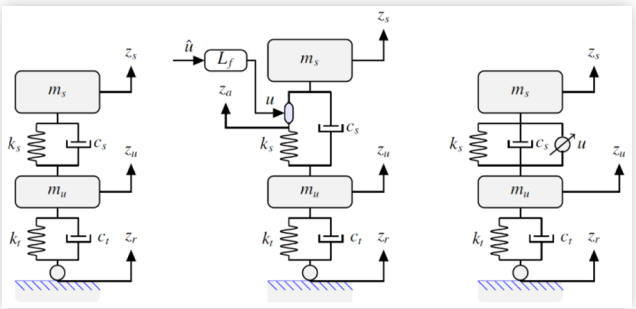

Mathematical Modelling and Problem Definition

Vehicle's Vertical Dynamics Modelling

A full car model for vehicle's vertical dynamics with active force elements is shown in Fig. 2. To develop a linear state-space model, we assume small deflections in pitch and roll directions. With this assumption, we write the motion equations of the sprung mass can as:

$$\begin{aligned} M_s\ddot{x}_s &= F_1+F_2+F_3+F_4 \\ I_p\ddot{\theta} &= -a\left(F_1+F_2\right)+b\left(F_3+F_4\right) \\ I_r\ddot{\phi} &= d\left(F_1+F_3\right)-d\left(F_2+F_4\right) \end{aligned} \tag{1}$$

The force provided by i^{th} suspension is denoted by F_i and can be expressed as sum of spring, damping and active force at the corner.

$$F_i = c_i\left(\dot{x}_{ui}-\dot{x}_{si}\right)+k_i\left(x_{ui}-x_{si}\right)+f_i \qquad \forall\ i\in\{1,2,3,4\} \tag{2}$$

Note that 1 → *Front Left* (*FL*), 2 → *Front Right* (*FR*), 3 → *Rear Left* (*RL*), 4 → *Rear Right* (*RR*). f_i is the active force

FIGURE 2 Full Car Active Suspension Model [5]

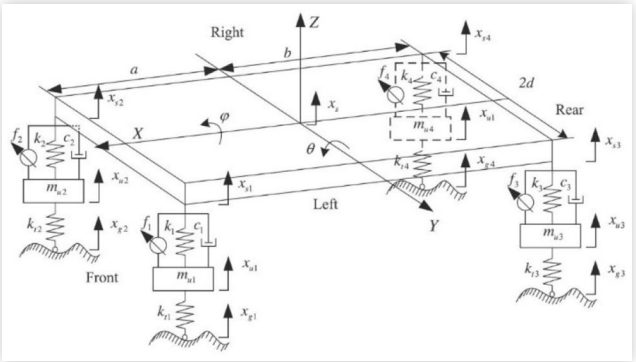

exerted by the i^{th} actuator; x_{si} can be expressed in terms of x_s, θ, ϕ as follows.

$$\begin{aligned} x_{s1} &= x_s - a\theta + d\phi, \\ x_{s2} &= x_s - a\theta + d\phi, \\ x_{s3} &= x_s - b\theta + d\phi, \\ x_{s4} &= x_s - b\theta + d\phi \end{aligned} \tag{3}$$

We write the equation of motion of the unsprung mass m_{ui} as follows

$$\begin{aligned} m_{ui}\ddot{x}_{ui} &= k_{ti}\left(x_{gi} - x_{ui}\right) - F_i \\ &= k_{ti}\left(x_{gi} - x_{ui}\right) - c_i\left(\dot{x}_{ui} - \dot{x}_{si}\right) - k_i\left(x_{ui} - x_{si}\right) - fi \end{aligned} \tag{4}$$

TABLE 1 Glossary for model parameters

M_s	Vehicle sprung mass
I_p	Pitch Inertia
I_r	Roll Intertia
x_s	Sprung mass displacement
θ	Pitch angle
ϕ	Roll angle
$\ddot{x}_s$	Vertical acceleration
$\ddot{\theta}$	Pitch acceleration
$\ddot{\phi}$	Roll acceleration
x_{si}	Sprung mass displacement
x_{ui}	Unsprung mass displacement
$\dot{x}_{si}$	Linear velocity of sprung mass
$\dot{x}_{ui}$	Linear velocity of unsprung mass
k_i	i^{th} Suspension Stiffness Coefficient
c_i	i^{th} Suspension Damping Coefficient
f_i	Control effort of i^{th} actuator
x_{gi}	Height of the ground disturbance at i^{th} wheel
k_{ti}	Stiffness coefficient of the i^{th} tire
a	Distance between CG and front axis
b	Distance between rear axis
d	Vehicle's halftrack width

Defining the control input $u(t) = [f_1, f_2, f_3, f_4]^T$, the ground disturbance $\varpi(t) = [x_{g1}, x_{g2}, x_{g3}, x_{g4}]^T$, and the state vector $x(t) = \left[x_s, \dot{x}_s, \theta, \dot{\theta}, \phi, \dot{\phi}, x_{u1}, \dot{x}_{u1}, x_{u2}, \dot{x}_{u2}, x_{u3}, \dot{x}_{u3}\, x_{u4}, \dot{x}_{u4}\right]^T$, the linear state-space form of the full-car suspension model can be obtained as

$$\begin{aligned} \dot{x}(t) &= Ax(t) + E\varpi(t) + Bu(t) \\ y(t) &- Cx(t) + Du(t) \end{aligned} \tag{5}$$

where A, B, C, D and E are matrices with proper dimensions. Here, $y(t) = \left[\dot{x}_s, \ddot{x}_s, \dot{\theta}, \ddot{\theta}, \dot{\phi}, \ddot{\phi}, x_{u1}\dot{x}_{u1}, x_{u2}, \dot{x}_{u2}, x_{u3}, \dot{x}_{u3}, x_{u4}, \dot{x}_{u4}\right]^T$ denotes the output vector in the state modelling of the vehicle suspension model.

Problem Statement

From the research and findings of Section I, we reinvestigate the potential of the low bandwidth hydraulic actuators in improving vehicle comfort. We aim to do so by analysing the effects of low frequency active force inputs to the vehicle model, see Fig. 2. We outline the objective of our investigation as follows:

Problem 1

Given a hydraulic actuation system with an operational bandwidth of 5 *Hz* and actuator saturation limit of 5000*N*. Determine if force inputs with frequency $\omega_f < 5$ *Hz* and force amplitude $A_f \leq 5000N$, can affect the ride characteristics of a vehicle installed with such an actuation system.

In our analysis, we consider a vehicle model with nominal parameters as listed in Table 2. Vehicle is moving at a speed of $v = 10\ ms^{-1}$ over a road surface resembling the power spectral density of a pink noise. A commonly used estimation of power spectral density is given in [11]

$$S_{x_g}(\omega) = \frac{1}{v} A_r \left(\frac{2\pi\omega}{v}\right)^n \tag{6}$$

Where A_r = constant roughness factor [*m*], ω = excitation frequency [*Hz*], and v = constant vehicle velocity $\left[\frac{m}{s}\right]$. One dimensional signal with $n = -1$ are usually called pink noise. For appropriate value of A_r, the power spectral density of the pink noise road is plotted in Fig. 3. For time step of 0.01 *seconds*, i.e., sampling frequency of 100*Hz*, we compute the time signals of road input as shown in Fig. 3.

As it is evident from Fig. 3, the frequency content of pink noise road lies predominantly in the frequency range $\omega \in [0, 30]$ *Hz*.Resulting body motion due these vibrations need to be controlled using hydraulic actuators. As per Problem 1., the operational bandwidth of actuator is limited to 5 *Hz*. So, majority frequency content of the force exerted by actuator will lie in this bandwidth. Moreover, compliance of suspension mounts at the top of actuator cylinder will also filter out the high frequency section of the input force. Analyzing vehicle's ride response to control inputs with frequency in this bandwidth will provide necessary insights to answer the problem. Hence, the control input ($f_i(t)$) at each corner can be written as follows:

$$f_i(t) = A_f \sin\left(2\pi\omega_f t\right), \quad \omega_f \in [0,5]Hz \tag{7}$$

TABLE 2 Selected parameter values for full-car model

m_{ui} (*kg*)	m_s (*kg*)	k_i (kNm^{-1})	c_i ($Nm^{-1}s$)	k_{ti} (kNm^{-1})
40	1550	18	1.4	220
I_r (kgm^2)	I_p(kgm^2)	a (*m*)	b (*m*)	d (*m*)
660	2080	1.5	1.8	1

FIGURE 3 Power Spectral Density of Pink Noise Road Input

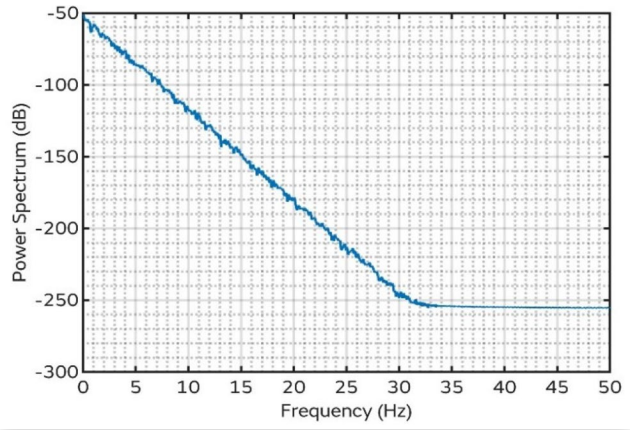

FIGURE 4 Time-series plot of Pink Noise Road Input

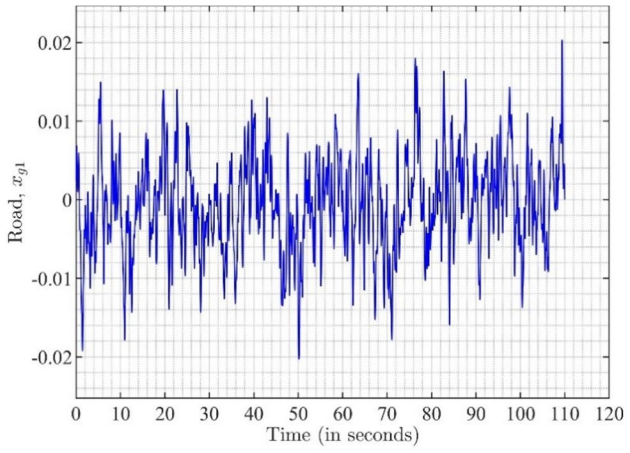

In our analysis, we excite the vehicle with a control input as given in (7). We run ten simulations through which we try to investigate the effect of control input's amplitude and frequency on the vehicle ride. Table 3 shows the amplitude and frequency of the control input we applied to our vehicle model.

Rear-left and rear-right wheels are excited with a delayed road signal. The delay is computed as $\delta = \frac{Wheelbase}{Speed} = \frac{a+b}{v} = \frac{3.3}{10} s = 0.33s$. This delay was also accounted in the application of input force to the front and rear vehicle corners.

TABLE 3 Control input parameters (A_f, ω) *used in simulations*

$A_f(N)\rightarrow$ / $\omega_f(Hz)\downarrow$	1000	2000	3000	4000	5000
1	×	×	✓	×	×
2	×	×	✓	×	×
3	×	×	✓	×	×
4	×	×	✓	×	×
5	✓	✓	✓	✓	✓

Model Verification and Simulation Results

We run simulations for time durations of T_{sim} = 110s to assess the vehicle's ride response to the pink noise road input. We analyse the frequency spectrum of sprung mass's acceleration in vertical, pitch and roll direction, i.e., $\ddot{x}_s, \ddot{\theta}$ and $\ddot{\phi}$ respectively, by computing the Fast Fourier Transform of the logged time-domain signals. The observations from our analysis are as follows.

Observations / Results

The simulations are grouped into two major categories:

1. A set of different Control Input Frequencies (1Hz, 2Hz, 3Hz, 4Hz, 5Hz) applied for a singular Force Input (3000 N) and compared also with the passive response.
   a. As seen in Fig. 5, in case of *Vertical acceleration*, different control input frequencies for the vehicle model results in spikes in the ride response at the input frequencies only.
   b. As seen in Fig. 6, in case of *Pitch Acceleration*, different control input frequencies for the vehicle model results in spikes in the ride response at the input frequencies only.
   c. Fig. 8 represents the *Roll Acceleration* amplitude relative to the passive roll acceleration response across the frequency range. Five data points have been highlighted at the frequencies of interest. This, in addition to the data presented in Fig. 7, shows significant improvement in roll response in the range near the frequency of 2 Hz. The relative roll acceleration values cross the unit line near the frequency of 5 Hz, indicating better response from the passive system.

FIGURE 5 Frequency response (FFT) of Vertical Acceleration under different frequency (ω_f) of input force with A_f = 3000N

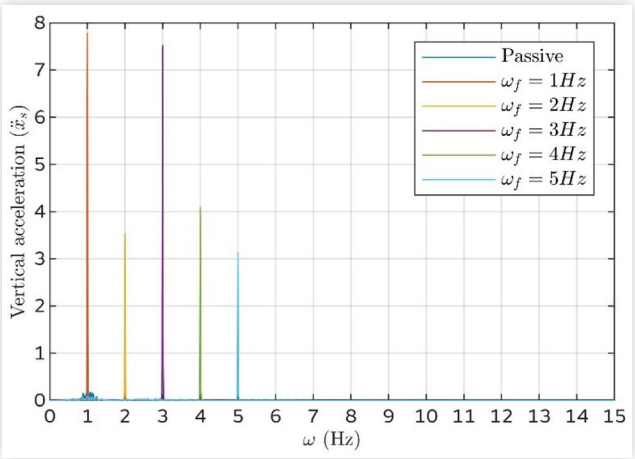

FIGURE 6 Frequency response (FFT) of Pitch Acceleration under different frequency (ω_f) of input force with A_f = 3000N

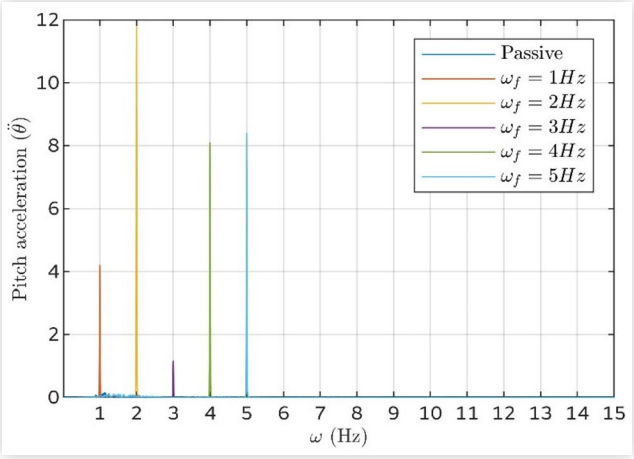

FIGURE 7 Frequency response (FFT) of Roll Acceleration under different frequency (ω_f) of input force with A_f = 3000N

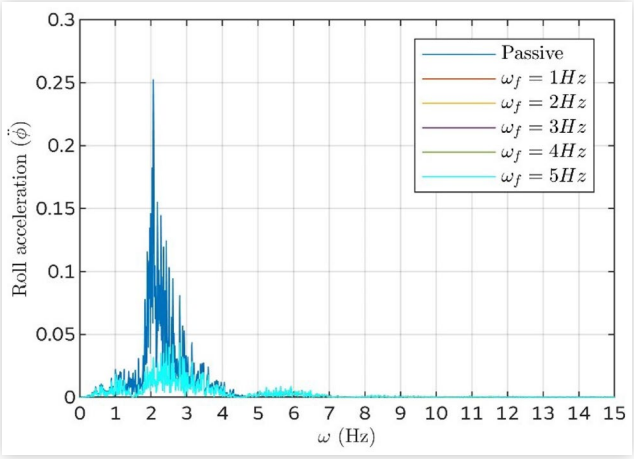

FIGURE 8 Comparison of Roll acceleration response at ω = 1, 2, 3, 4, 5, under different input force frequency ω_f with A_f = 3000N

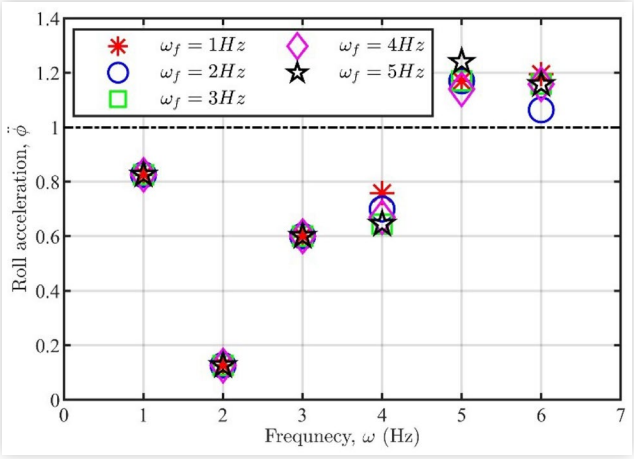

2. A set of different Force inputs (1000 N, 2000 N, 3000 N, 4000 N, 5000 N) at a particular Control Input Frequency (3 Hz) and compared also with the passive response.
   a. Fig. 9 represents the Frequency response of Vertical acceleration. Fig. 10 zooms in at 5 Hz from Fig. 9. From the figures, it is evident that the ride response changes at the input frequency only which is constant for this set of simulations and the amplitude of the spikes correspond to the magnitude of the Force inputs.
   b. Fig. 11 represents the Frequency response of Pitch acceleration Fig. 12 zooms in at 5 Hz from Fig. 11. From the figures, it is evident that the ride response changes at the input frequency only which is constant for this set of simulations and the amplitude of the spikes correspond to the magnitude of the Force inputs.

FIGURE 9 Frequency response (FFT) of Vertical Acceleration under different amplitude (A_f) of input force with ω_f = 5Hz

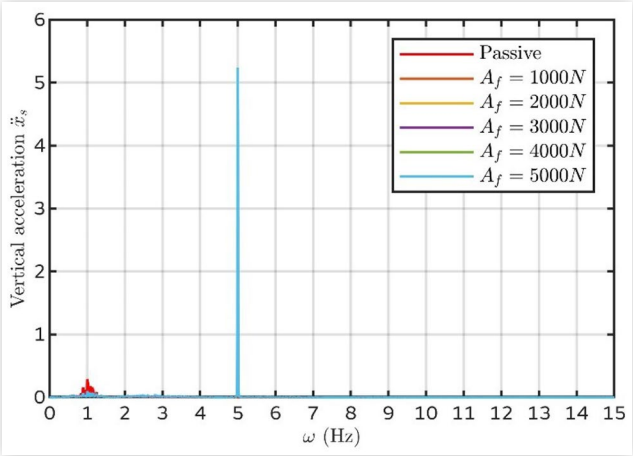

FIGURE 10 Magnified FFT of Vertical Acceleration at ω = 5Hz, under different amplitude (A_f) of input force with ω_f = 5Hz

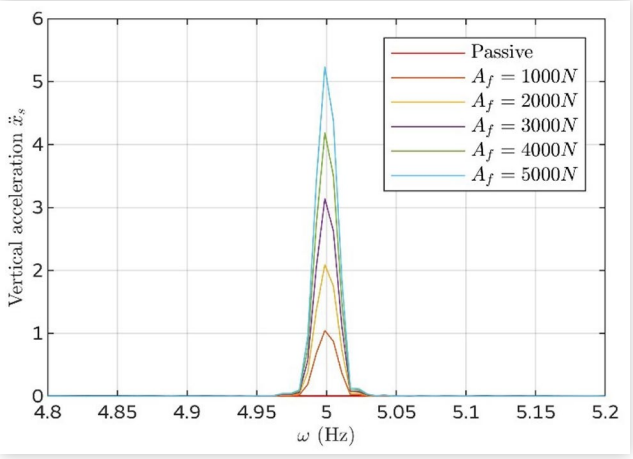

FIGURE 11 Frequency response (FFT) of Pitch Acceleration under different amplitude (A_f) of input force with ω_f = 5Hz

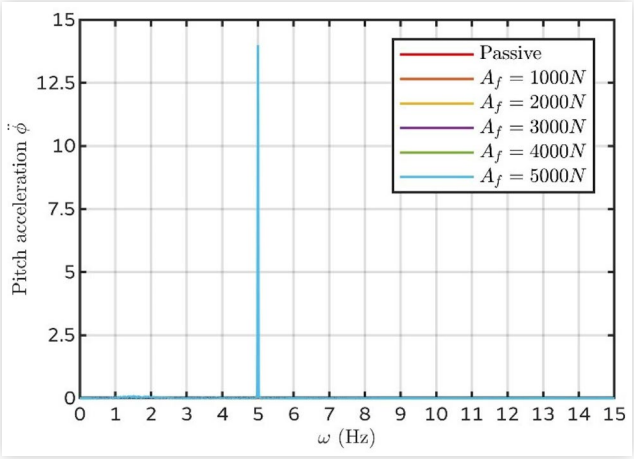

FIGURE 12 Magnified FFT of Pitch Acceleration at ω = 5Hz, under different amplitude (A_f) of input force with ω_f = 5Hz

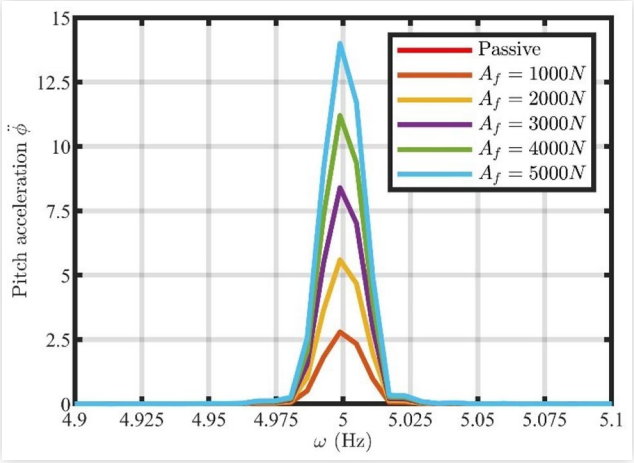

c. Fig. 14 represents the Roll acceleration amplitude relative to the passive roll acceleration response across the frequency range. Five data points have been highlighted at the frequencies of interest. This, in addition to the data presented in Fig.13, shows significant improvement in roll response in the range near the frequency of 2 Hz. The relative roll acceleration values cross the unit line near the frequency of 5 Hz, indicating better response from the passive system.

FIGURE 13 Frequency response (FFT) of Roll Acceleration under different amplitude (A_f) of input force with ω_f = 5Hz

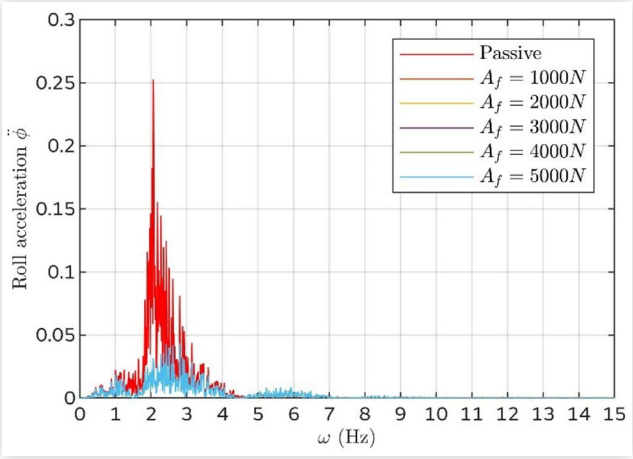

FIGURE 14 Comparison of Roll acceleration response at ω = 1,2,3,4,5, under different input force amplitude A_f with ω_f = 5Hz

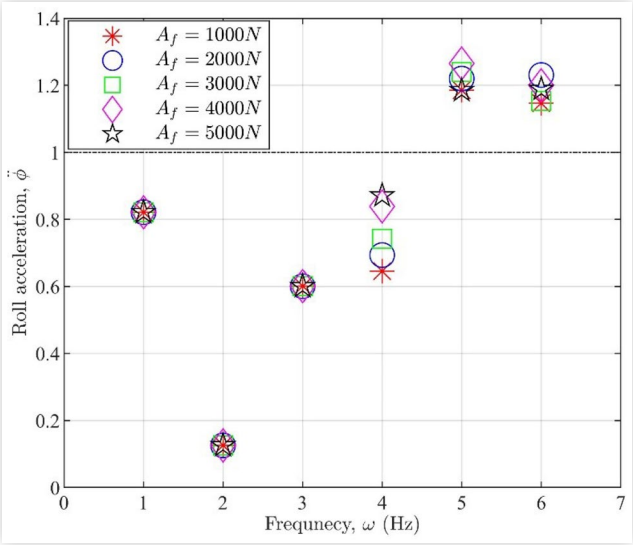

Conclusion and Future Work

Based on the simulation results, it is evident that a force input of a particular frequency does not affect the ride response at any other frequency. This means that the active force signal is restrained to the operational frequency bandwidth of the actuator. Owing to this

constraint, even the very advanced and sophisticated control strategies would not be effective for improving the ride response at higher frequencies. This leads to the conclusion that the ride response of a vehicle cannot be affected, and thus improved, by an actuator beyond its operational bandwidth. To be able to achieve the desired response, more developed actuators with a wider bandwidth, that encompass the required frequency range, are necessary.

This limitation of Hydraulic Actuators generates a need for developments in technologies such as Electromagnetic Actuators, which have a much wider operational frequency bandwidth as compared to Hydraulic Actuators. Major focus should be on reducing the weight and costs of Electromagnetic Actuator components.

Majority of the research on this topic, including this paper, is built upon linear vehicle models. The non-linearity in vehicle dynamics have not been taken into account. Going forward, a similar test strategy can be used on non-linear vehicle models which could give us more insight into the possibility of controlling the ride response at higher frequencies.

References

1. Multimatic, "Multimatic's Breakthrough TrueActive™ Damper Technology Featured on Ferrari Purosangue," September 13, 2022, accessed July 15, 2023, https://www.multimatic.com/press/multimatics-breakthrough-trueactive-damper-technology-featured-on-ferrari-purosangue.
2. Crosse, J., "How Ferrari's SUV Tech Redefines Active Suspension?" Autocar, October 10, 2019, accessed July 15, 2023, https://www.autocar.co.uk/car-news/technology/how-ferraris-suv-tech-redefines-active-suspension.
3. Baker, M., "Hydraulic vs. Pneumatic vs. Electric Actuators," York Precision, September 23, 2019, accessed July 15, 2023, https://yorkpmh.com/resources/hydraulic-vs-pneumatic-vs-electric-actuators/.
4. Koch, G., Fritsch, O., and Lohmann, B., "Potential of Low Bandwidth Active Suspension Control with Continuously Variable Damper," *Control Engineering Practice* 18, no. 11 (2010): 1251-1262, doi:https://doi.org/10.1016/j.conengprac.2010.03.007.
5. Jing, H., Wang, R., and Bao, J., "Robust Finite-Frequency H∞ Control of Full-Car Active Suspension," *Journal of Sound and Vibration* 441 (2019): 221-239, doi:https://doi.org/10.1016/j.jsv.2018.06.047.
6. Wasiwitono, U. and Nyoman Sutantra, I., "Constrained H∞ Control for Low Bandwidth Active Suspensions," in *AIP Conference Proceedings*, 2017, https://doi.org/10.1063/1.4994435
7. Gohrle, C., Schindler, A., Wagner, A., and Sawodny, O., "Road Profile Estimation and Preview Control for Low-Bandwidth Active Suspension Systems," *IEEE/ASME Transactions on Mechatronics* 20, no. 5 (2015): 2299-2310, doi:http://doi.org/10.1109/TMECH.2014.2375336.
8. Asadi, E., Khajepour, A., and Khamesee, B., "A New Low-Profile Electromagnetic-Pneumatic Actuator for High-Bandwidth Applications," *IEEE/ASME Transactions on Mechatronics* 23, no. 5 (2018): 2207-2217, doi:https://doi.org/10.1109/TMECH.2018.2854791.
9. Kruczek, A. and Stribrsky, A., "A Full-Car Model for Active Suspension - Some Practical Aspects," in *Proceedings of the IEEE International Conference on Mechatronics*, Istanbul, Turkey, 2004, http://doi.org/10.1109/ICMECH.2004.1364409
10. Pyper, M., Schiffer, W., and Schneider, W., *ABC-Active Body Control* (Ausburg: Verlag Moderne Industrie, 2003)
11. Hrovat, D., "Survey of Advanced Suspension Developments and Related Optimal Control Applications," *Automatica* 33, no. 10 (1997): 1781-1817, doi:https://doi.org/10.1016/S0005-1098(97)00101-5.

Contact Information

Please address all queries to Jaguar Land Rover Technology and Business Solutions India Private Limited, Brigade Tech Garden, 1st Cross Road, Brookfield, Karnataka, India - 560037
aagraw14@jaguarlandrover.com

ISSN 0148-7191